Ultrafast Direct Photoacid−Base Reaction

Liat Genosar, Boiko Cohen, and Dan Huppert*

School of Chemistry, Raymond and Beverly Sacler Faculty of Exact Sciences, Tel-Aviv University, Ramat-Aviv, Tel-Aviv 69978, Israel

Received: January 27, 2000; In Final Form: April 24, 2000

We have measured the direct proton-transfer rate between a photoacid, 8-hydroxypyrene-1,3,6- trisulfonate (HPTS) and a base, acetate anion in water and in D_2O, using a pump-probe technique with ∼150 fs time resolution. The acid−base reaction can be formulated by the kinetic scheme ROH* + B^- → RO^-* + BH, where ROH* and RO^-* are the excited-state protonated and deprotonated forms of HPTS, respectively, and B^- and BH are the deprotonated and protonated species of the acetate base, respectively. We have analyzed the experimental data within the framework of the diffusive model. We assume that both species are spherically symmetric and interact via a screened Coulomb potential of mean force. The reaction occurs with a certain rate whenever ROH* and B^- diffuse together and come into contact. Our data analysis of H_2O and D_2O solutions of 0.5−4 M sodium acetate shows a good agreement with the diffusive model. The intrinsic rate constants at contact of the reactive species were found to be 1.6×10^{11} and 4×10^{10} M^{-1} s^{-1} for H_2O and D_2O solutions, respectively. At 4 M salt concentration, the reaction rate is about 3 ps, one of the fastest intermolecular chemical reactions observed by time-resolved techniques.

Introduction

Proton-transfer reactions are a common example of acid−base reaction. Hydroxyarene molecules become strong acids in the first electronically excited state.[1−11] Light serves as an ultrafast trigger for proton transfer to solvent (PTTS). 1-Naphthol, 2-naphthol, and naphthol derivatives undergo an enhancement of acidity when excited to their first electronically excited singlet state.[3] Many photoacids exhibit acid−base equilibrium in their excited state. In these cases both proton dissociation and recombination occur reversibly on the excited-state potential surface.[12−15]

Besides their transient nature, such photoacids completely resemble ground-state proton acids. Thus, similar to ground-state acids, one can characterize the strength of a photoacid by assigning an excited-state equilibrium constant (K_a^*) to the proton dissociation reaction. In such a treatment, both proton dissociation and recombination reactions should be compared to the excited-state lifetimes of both the protonated and deprotonated forms of the photoacid.

A particularly convenient and stable photoacid is 8-hydroxypyrene 1,3,6-trisulfonate trivalent anion (pyranine, HPTS). It was experimentally shown with this molecule[13−15] that geminate recombination slows the apparent proton dissociation rate by virtue of being reversible in the excited state. The fingerprint of reversible pair kinetics is the observation of a long time, $t^{-3/2}$ dependence of the survival probability of the HPTS molecule.[15] After a proton is transferred to water it has a finite probability to recombine geminately with the RO^- anion. The reversible dissociation process is described by a two-step model where the chemical step of the bond breaking is followed by the diffusive motion of the proton around the RO^- species. The Debye−Smoluchowski equation (DSE) is successfully used for a quantitative description of the process. The introduction of low concentrations of moderate bases to the photoacid solution results in the reduction of the geminate recombination yield.[16] The bases react with the geminate proton before it recombines with the anion and hence reduce the probability for the proton to recombine with its geminate anion.

Most chemists are content in describing the kinetics of chemical reactions in solution by classical rate equations. In this approach, the time course of bulk concentrations is assumed to obey a set of ordinary differential equations. A particular case of importance throughout chemistry is that of diffusion-limited reactions with time-dependent reaction rate coefficients.[2,17] Fluorescence quenching is the process of most of the experimental studies of diffusion-controlled reactions, in which the time dependence of the quenching rate coefficient is manifested by a nonexponential decay of the fluorescence of the donor in the presence of the quencher.

Another class of experiments that can be formulated by diffusion formalism is the proton transfer from a photoacid to the solvent and the subsequent geminate recombination process.

In a previous study[16] we have measured the effect of proton scavenging from solvent on the reversible excited-state proton-transfer and geminate recombination reactions. When a proton scavenger is introduced to the solution, the geminate recombination process diminishes owing to the competition with the homogeneous scavenging reaction. The scavenging reaction may be incorporated into the DSE by the introduction of an additional sink term independent of time and position. When the proton scavenger concentration is high enough, it can react directly with the excited-state proton emitter and abstract a proton.

Recently Pines and co-workers[18] extended the concentration range of the proton base in aqueous solutions and measured the direct proton transfer between a photoacid and a base. When the base concentration is large enough, the direct proton-transfer reaction rate exceeds the proton-transfer rate to the solvent. For a diffusive model, in the limit of diffusion the steady-state second-order rate constant in units of M^{-1} s^{-1} is given by k_D =

* Corresponding author. Fax: 972-3-6407012. E-mail: huppert@chemosf1.tau.ac.il.

10.1021/jp000317l CCC: $19.00
Published on Web 07/01/2000

$4\pi N'Da$, where $N' = N_A/1000$ (N_A is the Avogadro number). D is the mutual diffusion constant of the reactants, and a is the contact radius. For $a = 7$ Å and $D = 10^{-5}$ cm^2/s, the pseudo first-order reaction rate for 1 M base is $k_D \cong 7 \times 10^9$ s^{-1}. At 1 M, the rate competes with the rate of proton transfer to the solvent of medium strong photoacids like HPTS, 2-naphthol, and 2-naphthol sulfonate derivatives like 2-naphthol-3,6-disulfonate and 2-naphthol-6,8-disulfonate.

The rate of neutralization of acids by strong bases has been considered to be an ultrafast event.[19] Studies in the past have shown that these reactions proceed with nearly diffusion-controlled efficiency. The diffusion-controlled rate constant, k_D, provides a rough estimate of the actual proton-transfer rates. Pines and co-workers have shown that at very high base concentration, like 8 M of aqueous solution of potassium acetate, the measured rate provided a good estimation for the intrinsic proton-transfer rates for several photoacids. The intrinsic rate constant for direct proton transfer from excited HPTS to acetate base was estimated to be 7×10^{10} s^{-1}.[19]

Recently femtosecond fluorescence up-conversion technique was applied by Tran-Thi and co-workers[20] to study the excited-state proton-transfer dynamics from HPTS to water. They found that the fluorescence decay consists of three time components. A mechanism for proton transfer, which involves three successive steps, was proposed. The first step of ~0.3 ps is attributed to solvation of HPTS in the excited state. The second step of 2.2 ps involves a hydrogen bond formation between ROH* and a specific water molecule. The last process involves the proton dissociation and diffusion at a rate of (87 ps)$^{-1}$.

In this study we have measured, by the femtosecond pump−probe technique, the direct proton transfer from excited HPTS to acetate base with ~150 fs time resolution in aqueous solution. The reaction rate was measured in the concentration range of 0.5−4 M sodium acetate (NaAc). We used a diffusive approach to analyze the experimental data. We found a good agreement between the model calculation and the experimental data. At the highest concentration (4 M) the reaction rate is ~3 ps. This rate is so far one of the fastest intermolecular reaction monitored in solution.

Experimental Methods and Data Analysis

Femtosecond Pump−Probe Technique. Pump−probe experiments reported employed a laser system based on the design of ref 21. In brief, laser pulses (50 fs duration, centered near 800 nm with a pulse energy of ~600 μJ) at a 1 kHz repetition rate were generated by a Ti:sapphire-based oscillator (Coherent Mira seed) amplified by a multipass Ti:sapphire amplifier (Odin Quantronix). Each laser pulse was split into two parts: pump and probe. The probe portion was used to generate white-light continuum in a 2 mm sapphire disk. The probe light was obtained by wavelength selection of this continuum using interference filters producing approximately 3 nm of bandwidth. The pump portion of the light was chopped at 35 Hz and optically delayed by a translation stage. Samples were excited by the second harmonic of the amplified laser (~400 nm). In the course of this study we also used a 360 nm pulse, the fourth harmonic of an OPA at 1440 nm (TOPAS, Light Conversion) with an energy per pulse of ~5 μJ. Within the signal to noise of the experimental data, we were not able to find a significant difference between the two excitation wavelengths. The second harmonic at 400 nm or the 360 nm pulses were generated in a 0.5 mm β-BBO crystal. The cross correlation between the pump and the probe pulses is measured to be 250 fs at full-width at half-maximum (fwhm), indicating that after deconvolution our experimental time resolution amounts to about 150 fs.

Time-Correlated Single-Photon Counting. Time-resolved fluorescence was measured using the time-correlated single-photon counting (TCSPC) technique. As an excitation source, we used a CW mode-locked Nd:YAG-pumped dye laser (Coherent Nd:YAG Antares and a 702 dye laser) providing a high repetition rate (>1 MHz) of short pulses (2 ps fwhm). The TCSPC detection system is based on a Hamamatsu R3809, photomultiplier, Tennelec 864 TAC, Tennelec 454 discriminator and a personal computer-based multichannel analyzer (nucleus PCA-II). The overall instrument response was about 45 ps fwhm (using a standard convolution analysis with the instrument response function the time resolution of a single-exponent fluorescence decay is about 20 ps). Measurements were taken at 10 nm spectral width.

8-Hydroxypyrene-1,3,6-trisulfonate (HPTS) was dissolved as its trisodium salt (Kodak, >99% chemically pure), D_2O (~99%), sodium acetate A.R. purchased from Aldrich. HPTS sample concentrations were between 2×10^{-4} and 5×10^{-4} M. Deionized water had a resistance >10 MΩ. All chemicals were used without further purification. The solution pH was about 6. Steady-state fluorescence spectra of the samples were recorded on a SLM-AMINCO-Bowman 2 luminescence spectrometer and corrected according to manufacturer specifications. All experiments were performed at room temperature (ca. 24 ± 2 °C). To reduce heating and photodegradation effects, a rotating cell was used for the sample in the ultrafast laser pulse experiments.

Viscosity Measurements of Sodium Acetate−H_2O/D_2O Solutions. In order to correctly fit our experimental data, we needed an estimation for the mutual diffusion coefficient, D, of the ion pair HPTS (as ROH*)−Ac$^-$ (B^-), which is concentration dependent. On the basis of the Stokes relation, D is inversely dependent on the viscosity, η. Therefore we conducted viscosity measurements of aqueous and deuterated solutions of sodium acetate at several salt concentrations. We used the Ostwald viscometer in order to evaluate the magnitude of η. In this apparatus the viscosity is measured by noting the time required for the liquid to drain between the two marks in the capillary. This time is compared to a known standard sample using the relation $\eta/\eta^* = t/t^*$, where η and η^* are the viscosity values for the unknown sample and the standard, respectively, and t, t^* are the times taken by the unknown sample and the standard to pass the capillary. The viscosity measurements were taken at room temperature of 24 °C (297 K). For each solution we took three measurements and used their average value. On the basis of Weller et al.,[3] we estimated that that the mutual diffusion constant $D_{ROH} + D_{Ac^-}$ at low salt concentration is $D = 2 \times 10^{-9}$ m^2 s^{-1}. Table 1 shows the values of the measured relative viscosities.

The Diffusive Model. The direct proton-transfer reaction between the excited HPTS molecule (ROH*) and the acetate anion (B^-)

$$\mathrm{ROH^* + B^- \rightarrow RO^{-*} + BH} \qquad (1)$$

can be described by a diffusive model. The direct proton-transfer reaction rate is formulated by the Smoluchowski theory[22] for a static "target" molecule with a distribution c of diffusing scavenger molecules. The survival probability, $S(t)$, of ROH* surrounded by an equilibrium distribution of acetate anion of concentration c is assumed to satisfy

$$dS(t)/dt = -k(t)cS(t) \qquad (2)$$

where the time-dependent rate constant $k(t)$ is calculated from

the time-dependent solution of the Debye−Smoluchowski equation for a geminate pair. For an arbitrary potential, $U(r)$, it is not possible to solve the DSE analytically. Szabo has found an approximate expression for the time-dependent rate constant[23]

$$k(t) = \frac{4\pi D a_e k_0' e^{-\beta U(a)}}{k_0' e^{-\beta U(a)} + 4\pi D a_e}\left\{1 + \frac{k_0' e^{-\beta U(a)}}{4\pi D a_e} e^{\gamma^2 D t}\mathrm{erfc}[(\gamma^2 D t)^{1/2}]\right\} \quad (3)$$

where a is the contact radius, $\beta = 1/k_B T$, and $U(a)$ is the interaction potential between the reactants at the contact radius a in units of the thermal energy $k_B T$. Here we apply the screened Coulomb potential of Debye and Hückel[24]

$$\beta U(r) = -\frac{R_D}{r}\frac{\exp[-\kappa_{DH}(r-a)]}{1+\kappa_{DH} a} \quad (4)$$

where R_D and κ_{DH}^{-1} are the Debye and ionic-atmosphere radii, respectively

$$R_D \equiv |z_1 z_2| e^2/\varepsilon k_B T \quad (5a)$$

$$\kappa_{DH}^2 \equiv 8\pi e^2 c/\varepsilon k_B T \quad (5b)$$

$$\kappa_{DH} a \equiv B\sqrt{c} \quad (5c)$$

where $B = 3 \times 10^{-9}$ cm^{-1} mol$^{-1/2}$ for water, $z_1 = -1$, $z_2 = -3$ are the charges of the acetate and deprotonated HPTS, respectively, e is the electronic charge, ε is the static dielectric constant of the solvent, k_B is Boltzmann's constant, T is the absolute temperature, $c \equiv$ [NaAc] is the concentration of the univalent electrolyte, and a is the reaction contact radius. γ is given by

$$\gamma = a_e^{-1}\left(1 + \frac{k_0' e^{-\beta U(a)}}{4\pi D a_e}\right) \quad (6)$$

erfc is the complementary error function, k_0' is the rate constant of the reaction at contact, and $k_0 = k_0' N'$ is a second-order rate constant in M^{-1} s^{-1} units, where $N' = N_A/1000$ and $k_D = 4\pi D a_e N'$ is the diffusion-limited second-order rate constant in M^{-1} s^{-1} units. a_e is an effective radius given by

$$a_e^{-1} = \int_a^\infty e^{\beta U(r)} r^{-2}\, dr \quad (7)$$

The survival probability of ROH* surrounded by an equilibrium distribution of ions with initial condition $S(0) = 1$ is

$$S(t) = \exp(-c\int_0^t k(\tau)\, d\tau) \quad (8)$$

where c is the concentration of the acetate ion in our case and $k(t)$ is the time-dependent rate constant, given by eq 3.

The pump probe signal measured at 540 nm monitors the RO$^-$*(t) population. We used the relation [RO$^-$*(t)] = 1 − [ROH*(t)].

Results and Discussion

Spectral Shifts. The time-integrated emission of HPTS consists of two broad structureless bands centered at 22 600 cm^{-1} (440 nm) and 19 600 cm^{-1} (510 nm) assigned to ROH* and RO$^-$*, respectively.

In the experiments we used large concentrations of acetate salt. Introducing sodium acetate to aqueous solutions of HPTS at concentrations levels of a few moles might alter the solvent structure and affect several parameters that are important in determining the direct proton-transfer reaction rate and mechanism.

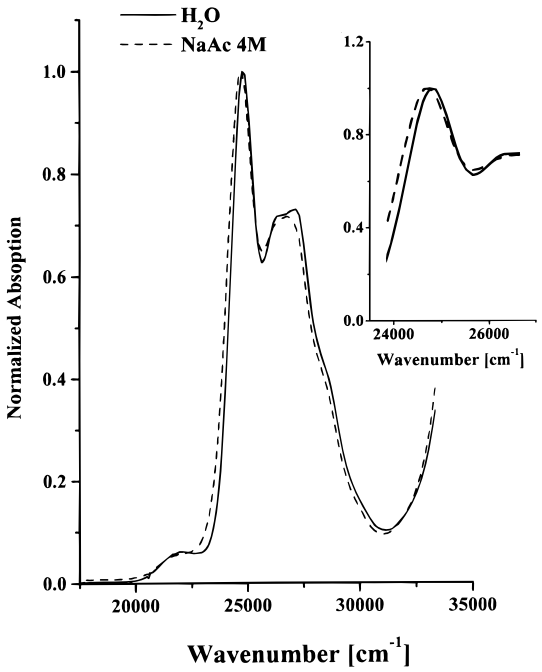

Figure 1. Ground-state absorption spectra of HPTS in pure water (solid line) and in aqueous solution of 4 M NaAc salt (broken line). Inset: Spectral enlargement of the electronic origin region.

Changes in both absorption and emission spectra of ROH and RO$^-$ in sodium acetate aqueous solutions might indicate preexisting complexes of acetate−ROH. We conducted steady-state spectral measurements of HPTS absorption, fluorescence, and excitation spectra in solutions containing sodium acetate of concentrations up to 4 M (Figures 1 and 2). In the case of preexisting ground-state complexation between ROH and B$^-$ to form a hydrogen bond complex, ROH···B$^-$, the apparent absorption and emission spectra of a HPTS solution are a superposition of two distinctive spectra. The first one is ROH surrounded only by the solvent (in our case, water molecules), and the second distinctive solvate includes a base molecule in the first solvation layer with a unique spectral shift due to a ROH···B$^-$ hydrogen bond. One can ascribe the equilibrium constant for the complexation reaction for both the ground and excited states

$$\mathrm{ROH{\cdots}S} + \mathrm{B}^- \overset{K_{eq}}{\rightleftharpoons} \mathrm{ROH{\cdots}B}^- + \mathrm{S}$$

where the broken line denotes hydrogen bonding.

In a previous study of spectral shifts of 5-cyano-2-naphthol,[25] we estimated that the hydrogen bond ROH···H$_2$O shifts the emission band to the red by about 1000 cm^{-1}. We expect that the magnitude of the spectral shift of a preexisting hydrogen bond complex ROH···B$^-$ would differ from that of water, and hence we should observe a distinctive change in either the absorption or the emission spectra. Examination of both absorption and emission spectra of HPTS in the presence of varying concentrations of NaAc shows that the spectra are only slightly red shifted and that at 4 M the shift is only 80 cm^{-1} (Figures 1 and 2). For comparison we also measured the fluorescence spectrum of HPTS in aqueous NaCl solutions up to 4 M. A similar bathochromic shift is also observed in NaCl solutions. These small spectral shifts at high salt concentrations

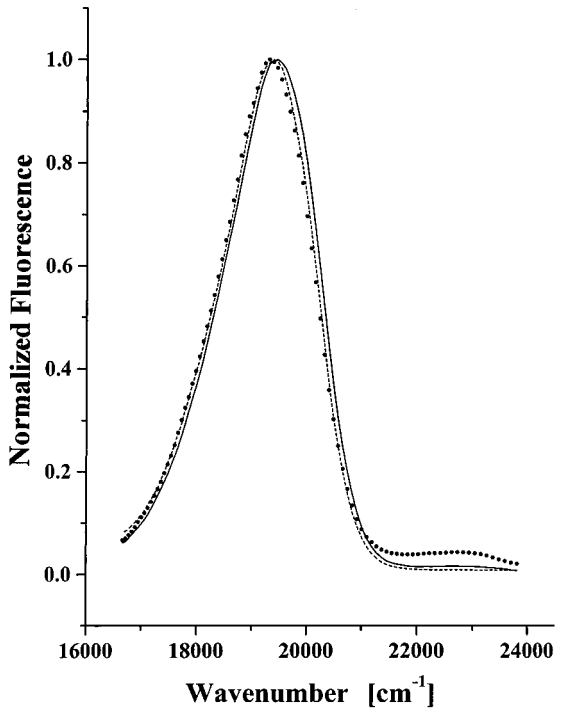

Figure 2. Steady-state emission spectra of HPTS in pure water (solid line), in aqueous solution of 4 M NaAc salt (broken line), and in aqueous solution of 4 M NaCl (dots). $\lambda_{excitation} = 404$ nm.

are probably due to electrostatic interactions of water−ion and HPTS−ion. We therefore conclude that in solutions of up to 4 M NaAc the concentration of such complexes is negligible.

Pump−Probe Measurements of HPTS in Neat Water. Figure 3a,b show the pump−probe signal of HPTS in water measured at 540 nm after excitation of the sample by a ∼100 fs pulse at 400 nm. The change in the probe pulse transmission, ΔT, changes signs from $\Delta T < 0$ to $\Delta T > 0$ at about 50 ps. The signal consists of three distinct time regimes, a short-time component of ∼700 fs, a second component of ∼3 ps, and a long-time component of about 100 ps. The computer fits to the signals with the above-mentioned time components are shown in Figure 3a,b as solid lines. Figure 3c shows the signal obtained for alkaline solution (pH ∼ 10) where the HPTS molecule is already in the ground state in its deprotonated form, RO^-. The signal is negative and assumes 70% of the absolute value within 300 fs, the time response of the system. The rest of the signal has a growth time of ∼700 fs. A 700 fs decay component is also seen in the signal of neutral solution where the ROH species are excited.

We attribute the positive part of the signal to absorption due to the optical transition $ROH(S_1) \rightarrow ROH(S_2)$. The negative component arises from the RO^-* stimulated emission due to transition to the ground state. The total signal at 540 nm is analyzed by

$$-\Delta T \propto \sigma_{ROH^*} S(t) - \sigma_{RO^-*}(1 - S(t)) \qquad (9)$$

where σ_{ROH^*} denotes the absorption cross section of the S_1 to a higher excited-state $S_1 \rightarrow S_n$ transition of ROH and σ_{RO^-*} denotes the emission cross section of RO^-*. $S(t)$ and $(1 - S(t))$ are the excited-state survival probabilities of ROH* and RO^-*, respectively. The short components arise from changes in both σ_{ROH^*} and σ_{RO^-*}, and their origin is discussed in the next section. We checked whether the signal is linear with the power of the excitation pulse. We changed the laser power by a factor of seven by reducing the pump energy from 5 μJ to ∼0.7 μJ. The power dependence measurements revealed that the signal shape is independent of the excitation power and the signal intensity is linear with the excitation power.

The Origin of the Short Components. The time-resolved fluorescence signal using the up-conversion technique measured by Tran-Thi and co-workers[20] also exhibited three time components with slightly shorter life times than we found in this study. The fastest component of 0.3 ps was attributed to solvation dynamics and the 2.2 ps component to a specific solute−solvent hydrogen bond formation.[20] The long component of 87 ps fits approximately to the fluorescence decay of ROH* and to the growth of the fluorescence of RO^-* measured by time-correlated single-photon counting techniques.[12−14] The changes in the values of the decay times between the two studies may arise from the differences in the laser power used and the two methods of measurement.

Spectroscopic measurements are used to quantify solvent effects on solute molecules. Solvent-induced spectral shifts are usually attributed to solvent (S) polarity/polarizability effects and its hydrogen bond (HB) donating or accepting properties.

In recent studies[25,26] we had quantified the relative contributions of the various solvent parameters to the spectral shift of 2-naphthol and 5-cyano-2-naphthol in several solvents. When excited to S_1, both its dipole moment and acidity increase dramatically. Therefore, the solvent rearranges to accommodate the enhanced dipole (nonspecific solvation), and the HB strengthens considerably. It is likely that a decrease in HB length occurs in solution. In the time domain, one might expect two ultrafast solvation phases: one due to HB shortening and the second one from nonspecific solvent reorganization.

The solvatochromic shifts in *both* excited ROH* acid and RO^-* base emission are intimately related to HB formation and contribute to pK_a^*. Water emerges as a unique solvent for promoting acid dissociation owing to the combination of its high dielectric constant with its ability to act as both HB acceptor and donor.

The question arises whether the assignments of Tran-Thi and co-workers[20] of the fast components in the fluorescence signal are exclusive. The literature data shows that water solvation is fast and hydrogen bond formation or rapture in aqueous solutions are longer processes. Solvation dynamics measurements of coumarin 343 dye in water[27] and simulations[28,29] have shown that solvation is a bimodal process. An ultrafast component of less than 50 fs is followed by a 0.8 ps component. Recently we have found that the long component of solvation of rhodamine 800 dye in water is much longer than of coumarin and for water it is 7 ps and for D_2O 10 ps.[30] We attribute it to a hydrogen bond formation. These decay times are almost identical to water and D_2O dielectric relaxation times.[31] It is plausible that hydrogen-bond formation or breaking has a range of time scales depending on the nature of both solute and solvent and whether a weak hydrogen bond already exists as mentioned above. In photoacids like 2-naphthol and naphthol derivatives, the ground-state ROH species already exhibit a hydrogen bond.[25,26] Upon excitation of HPTS the change in the charge distribution and bond lengths will probably affect this preexisting hydrogen bond at much shorter times. If the time scale of this change is shorter than the long component of the solvation dynamics, then the assignment of the time components by Tran-Thi and co-workers[20] might be wrong. The fact that the short component of 700 fs exists in the signal of both ROH* and RO^-* (Figure 3a,c) is in favor of the assignment to nonspecific solvation. More experiments are needed to clarify this important

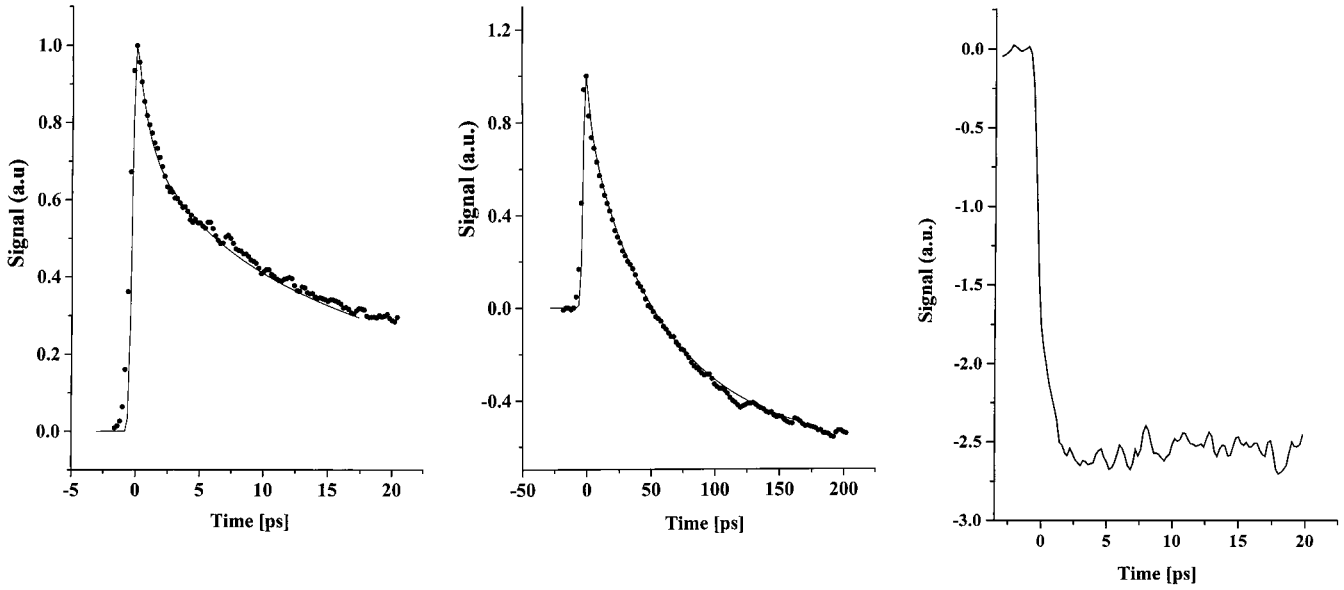

Figure 3. Pump−probe signal of HPTS in water along with the computer fits to a three-exponential decay function. The sample was pumped at 400 nm and probed at 540 nm: (a, left) short times, sample at neutral pH; (b, center) long times, sample at neutral pH; (c, right) sample excitation of the RO^- species, at pH = 10.

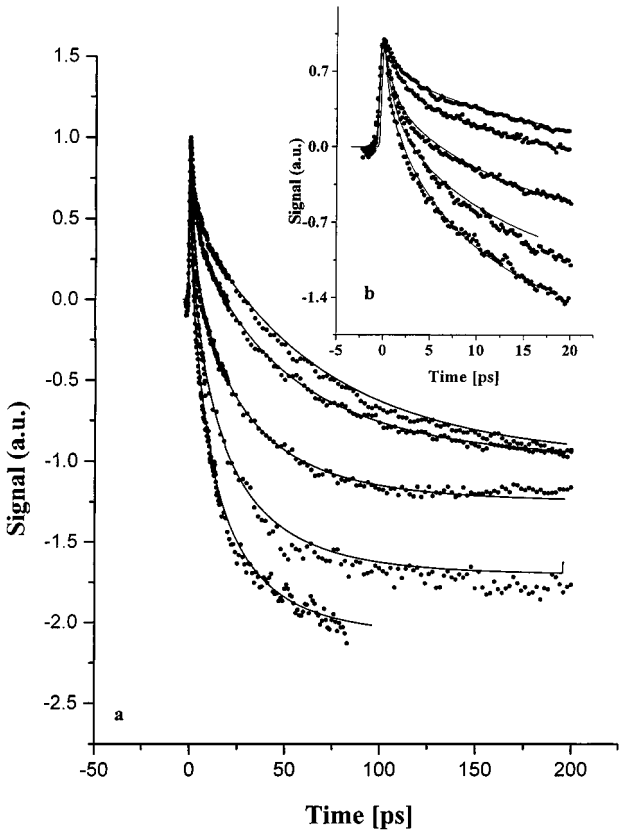

Figure 4. Pump−probe signal (dots) of HPTS aqueous solutions containing sodium acetate salt (NaAc) at several salt concentrations (top to bottom: 0.5, 1, 2, 3 and 4 M) along with computer fits (solid line) at two time scales. The samples were pumped at 400 nm and probed at 540 nm: (a) long times; inset, (b) short times.

point. At present we cannot conclusively assign which of the two fast components in the pump−probe signal shown in Figure 3a,b is due to specific hydrogen bonding.

The Direct Proton Transfer to the Acetate Base. Figure 4 shows the pump−probe signal measured at 540 nm of HPTS aqueous solutions containing sodium acetate salt (NaAc) at several salt concentrations. At concentrations of >0.1 M, the steady-state diffusion-controlled rate of the direct proton transfer

$$ROH^* + B^- \xrightarrow{k_D} RO^{-*} + BH \qquad (10)$$

is faster than the proton-transfer rate to water, $k_d \sim (120\ ps)^{-1}$.[13] At lower acetate concentrations the effect on the ROH* and RO^{-*} populations of direct proton transfer to a base is rather small. The direct proton transfer to the base increases the rate of RO^{-*} formation, which causes the large difference in the pump−probe signal, shown in Figure 4, in the presence of NaAc at concentrations >0.1 M.

We have used the diffusive reaction model at the Debye−Smoluchowski spherical-symmetric level to quantify the experimental data of direct proton transfer from excited HPTS ROH* to an acetate anion. Within the model there are several parameters that determine the actual dynamics D, $U(r)$, c, k_0 and a. The mutual diffusion constant of the reactants, D, was determined by Weller[3] as $D = D_{Ac-} + D_{HPTS} \cong 2 \times 10^{-5}\ cm^2\ s^{-1}$. $U(r)$, the repulsive potential is computed by the Debye−Hückel screening formula (eqs 3−4). For the contact radius a we used 7 Å, the accepted literature value for proton-transfer reaction.[3] It also resembles the actual size of HPTS and a water molecule in the first solvation shell surrounding it. k_0, the intrinsic proton-transfer reaction rate constant, is used as an adjustable parameter. In the fitting procedure of the experimental data its value was kept constant for all acetate concentrations 0.5−4 M. The pump−probe signal changes sign as time progresses. The relative amplitude of the positive and negative parts of the experimental signal is determined by the ratio of the cross sections of absorption $ROH(S_1) \xrightarrow{h\nu} ROH(S_2)$, σ_{ROH}, and the emission cross section of a photon at 540 nm, σ_{RO^-}, of RO^{-*}, which is formed by the direct proton-transfer reaction. From the data simulations we find at 540 nm a ratio: $\sigma_{ROH}/\sigma_{RO^-} \cong 1/2.8$.

In general, the signal at 540 nm was analyzed as follows

$$y = a_1 e^{-t/\tau_1} + a_2 e^{-t/\tau_2} + a_3 S'(t) - a_4(1 - S'(t)) \qquad (11)$$

where a_1, τ_1 are the amplitude and the lifetime of the fastest component (0.7 ps). a_2 and τ_2 are the parameters of the slower

TABLE 1: Fitting Parameters for Simulations of Experimental Results: HPTS in Aqueous Solutions Containing NaAc Salt at Different Concentrations[a]

NaAc concn (M)	a_4	a_1	τ_1 (ps)	a_2	τ_2 (ps)	D ($cm^2\,s^{-1}$) diff. coeff.	relative viscosity
0	0.67	0.30	0.7	0.35	3.0	2.2×10^{-5}	1.00
0.5	0.95	0.25	0.7	0.25	3.0	2.0×10^{-5}	1.07
1	0.92	0.25	0.7	0.25	3.0	1.9×10^{-5}	1.24
2	1.15	0.25	0.7	0.25	1.2	1.8×10^{-5}	1.64
3	1.55	0.25	0.7	0.25	1.0	1.0×10^{-5}	2.30
4	1.75	0.25	0.7	0.25	1.0	0.85×10^{-5}	3.00

[a] Fitting parameters according to eq 14 in the text. In all the fits the following values were kept constant: $k_0 = 1.6 \times 10^{11}$ ($M^{-1}\,s^{-1}$); $a_3 = 0.6$; $k_d = (100\text{ ps})^{-1}$.

component (for neat water 3.0 ps). $S'(t) = S(t)e^{-k_d t}$, $S(t)$ is the survival probability computed from eq 8, and k_d is the proton-transfer rate of HPTS to water ($k_d = (120\text{ ps})^{-1}$). The population of ROH* has a relatively short lifetime, since it also reacts with the water molecules and transfers the proton to the water in competition with the Ac^- base reaction. The product $a_3S'(t)$ gives the relative contribution of the ROH*(t) population to the signal. a_3 is related to the absorption cross section $ROH(S_1) \rightarrow ROH(S_n)$ (σ_{ROH}). $S'(t)$, the survival probability of the protonated form, converts to $(1 - S'(t))$, the deprotonated form survival probability by the proton-abstraction reaction. a_4 is related to the emission cross section of the transition $RO^-(S_1) \rightarrow RO^-(S_0)$, ($\sigma_{RO^-}$).

Table 1 gives the relevant parameters for the data fit. The computer fits to the experimental pump−probe signal for HPTS−sodium acetate water solutions (pumped at 400 nm and measured at 540 nm) are shown as solid lines in Figure 4. We get good fits to the experimental results for the value of $k_0 = 1.6 \times 10^{11}\ M^{-1}\ s^{-1}$ at all acetate concentrations. The pseudo first-order rate at 4 M sodium acetate is $\sim(3\text{ ps})^{-1}$. The fastest signal component that was found for neat water solution as 0.7 ps does not depend on the acetate concentration, while the second component of 3 ps reduces to ~1.0 ps at acetate concentrations ≥2 M.

Figure 5 shows the pump−probe signal of HPTS−D_2O pumped at 400 nm and measured at 540 nm in the presence of various concentrations of NaAc. The same mathematical procedure was used to fit the experimental data for the deuteron transfer in D_2O. Figure 5 shows as solid lines the fit to the D_2O measurements. Table 2 provides the relevant parameters of the D_2O computer fit. The value for the intrinsic deuteron-transfer rate constant at the contact radius $k_0^{D+} = 4 \times 10^{10}\ M^{-1}\ s^{-1}$, and the isotope effect is $k_0^{H+}/k_0^{D+} \cong 4$.

The isotope effect of the intrinsic rate constant for proton/deuteron transfer to water/D_2O of excited HPTS is ~3.[12−14] In contrast, the isotope effect of the back-reaction $RO^{-}* + H_3O^+ \rightarrow ROH* + H_2O$ is only 1.4, similar to the isotope effect of proton mobility.[32] The viscosity and dielectric relaxation isotope effects at room temperature are 1.2 and 1.25, respectively.[33] The large isotope effect found for the direct proton/deuteron transfer from HPTS to acetate indicates that the mechanism of both proton transfer to the solvent and the direct proton transfer to acetate exhibits similar rate-limiting steps. A relatively large isotope effect is expected in the actual proton/deuteron transfer along the hydrogen coordinate.[34,35]

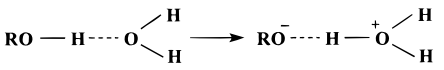

The Diffusive Model for Photoacid−Base Reactions. The analysis of the pump−probe data is based on the diffusive model, given in eqs 2−8. The free parameter of the data fit is the intrinsic proton-transfer rate constant, k_0, from the photoacid to the acetate anion. All other parameters are known from published literature values. For water we found an intrinsic second-order rate constant, $k_0 = 1.6 \times 10^{11}\ M^{-1}\ s^{-1}$. It is about 20 times larger than the diffusion-controlled rate constant $k_D = 4\pi D a_e N'$, where $D = 2 \times 10^{-5}\ cm^2/s$, $a_e \sim 4.5$ Å. In such a case the time-dependent rate constant, eq 3, changes drastically with time. Figure 6 shows the time dependence of $k(t)$ calculated

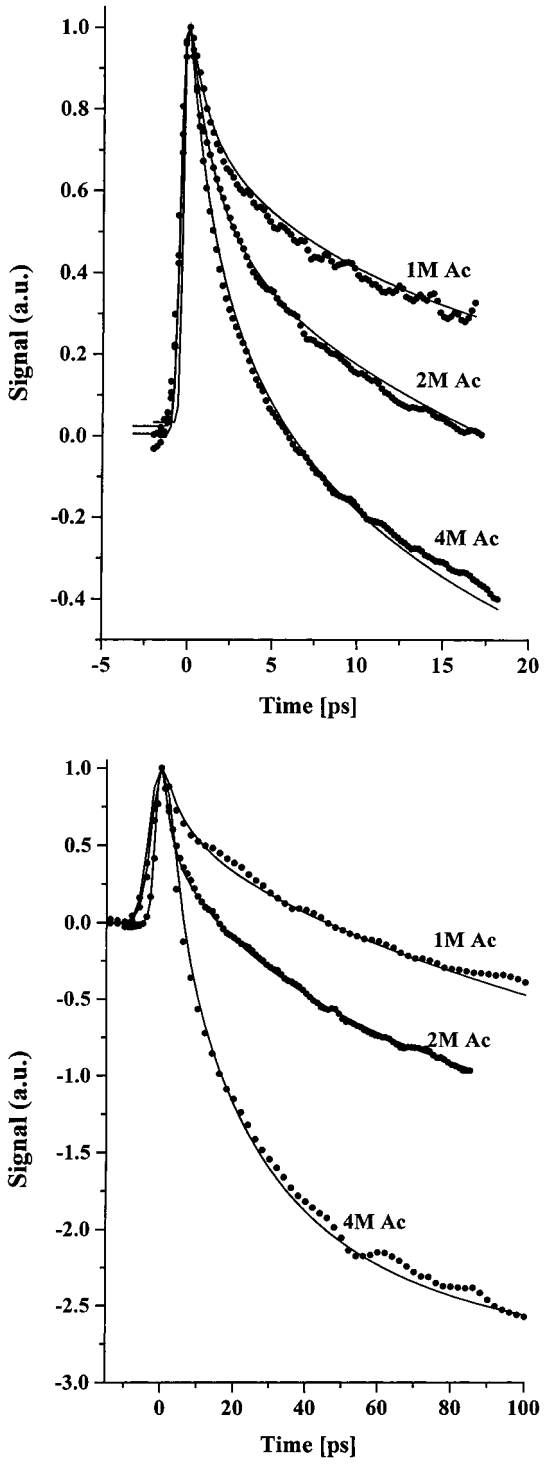

Figure 5. Pump−probe signal of HPTS−D_2O solutions in the presence of NaAc salt, at various concentrations, at two different time scales along with computer fits (solid line). The samples were pumped at 400 nm and probed at 540 nm: (a, top) short times; (b, bottom) long times.

TABLE 2: Fitting Parameters for Simulations of Experimental Results: HPTS in D_2O Solutions Containing NaAc Salt at Different Concentrations at Two Time Scales[a]

NaAc concn (M)	a_4	a_1	τ_1 (ps)	a_2	τ_2 (ps)	D ($cm^2 s^{-1}$) diff. coeff.	relative viscosity[b]
2.1. Short Times (20 ps)							
1	1.60	0.42	1	0.33	6.5	2.5×10^{-5}	1.33
2	1.75	0.42	1	0.33	2.5	2.0×10^{-5}	1.76
4	1.70	0.50	1	0.50	2.5	1.4×10^{-5}	3.26
2.2. Long Times (100 ps)							
1	1.60	0.42	1	0.33	6.5	2.5×10^{-5}	1.33
2	1.75	0.50	1	0.43	2.5	2.0×10^{-5}	1.76
4	1.75	0.50	1	0.50	2.5	1.4×10^{-5}	3.26

[a] Fitting parameters according to eq 14 in the text. In all the fits the following values were kept constant: $k_0 = 0.4 \times 10^{11}$ ($M^{-1} s^{-1}$), $a_3 = 0.6$, $k_d = (300 \text{ ps})^{-1}$. [b] The viscosity is related to water.

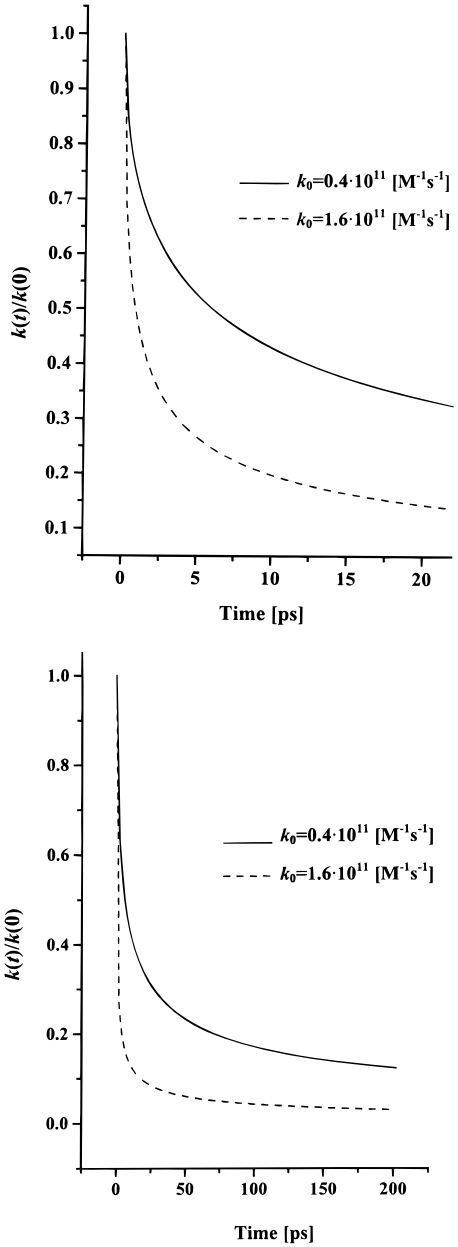

Figure 6. Comparing $k(t)$ at two time scales and different values for k_0, with $D = 2 \times 10^{-9}$ M^{-1} s^{-1} and $Z = -3$; (a, top) short times; (b, bottom) long times.

from eq 3 with the relevant parameters of the acid−base reaction. At $t = 0$ it assumes the value $k_0 e^{-\beta U(a)}$ (for 4 M NaAc,

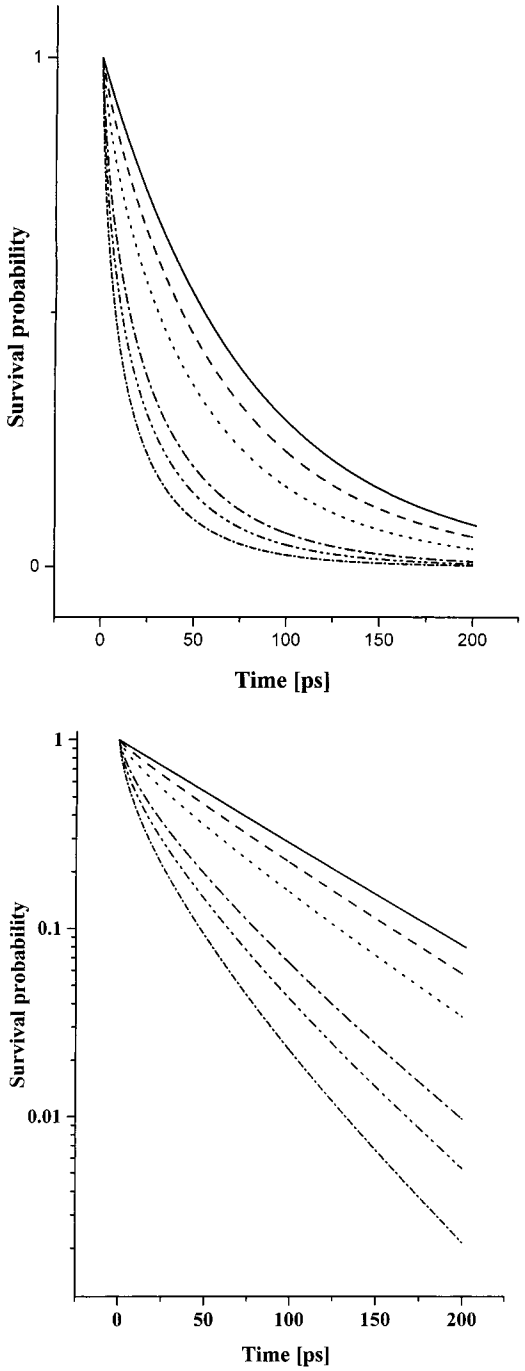

Figure 7. Calculated survival probabilities of ROH*, $S(t)$, at different NaAc concentrations (top to bottom: neat water, 0.5 M, 1 M, 2 M, 3 M, and 4 M). (a, top) linear scale; (b, bottom) semilog scale.

$e^{-\beta U(a)} \approx 0.5$, and $k_0 e^{-\beta U(a)} = 8 \times 10^{10}$ M^{-1} s^{-1}). The long-time asymptotic expression of $k(t)$ is given by eq 12

$$k = \lim_{t \to \infty} k(t) = \frac{4\pi D a_e k_0' e^{-\beta U(a)}}{k_0' e^{-\beta U(a)} + 4\pi D a_e} \qquad (12)$$

where $k_0' = k_0/N'$. In our case $k_0 e^{-\beta U(a)}$ is much larger than k_D (for 4 M NaAc $D \cong 0.7 \times 10^{-5}$ cm^2/s), and therefore $k \approx k_D$ ($k_D = 3 \times 10^9$ M^{-1} s^{-1}, more than 20 times smaller than its initial value).

The survival probability of ROH, $S(t)$, is calculated from eq 8 and is shown in Figure 7. Since $k(t)$ is time-dependent, $S(t)$ decays nonexponentially and $S'(t)$ decays exponentially at very

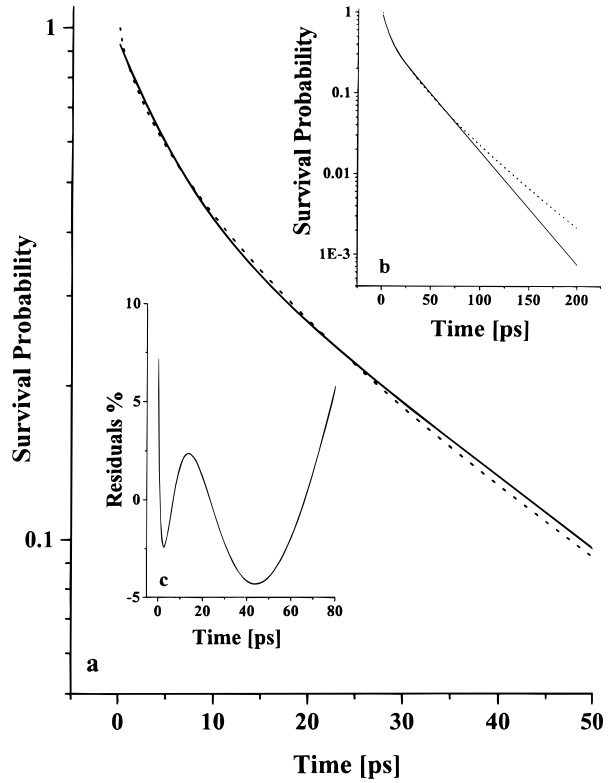

Figure 8. Survival probability of ROH*, $S(t)$, at 4 M NaAc (full line) along with a biexponential fit (broken line): (a) short times; inset, (b) long times; (c) residuals.

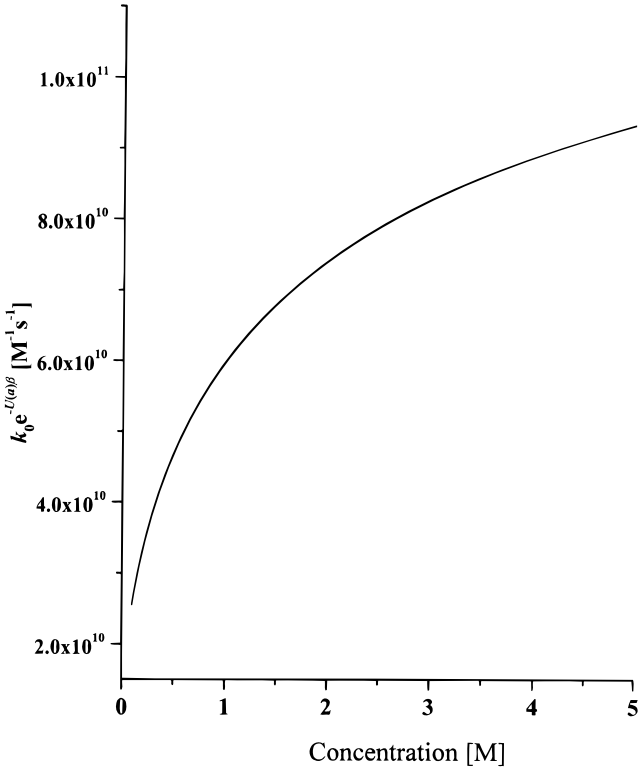

Figure 9. Concentration dependence of the initial rate constant.

long times. We compared the survival probability of ROH to a two-exponential function $y'(t) = \alpha e^{-k_1 t} + (1 - \alpha)e^{-k_2 t}$. Figure 8 shows such a comparison for 4 M NaAc aqueous solution. We found that the residuals, $R(t) = [(S'(t) - y'(t))/S'(t)'] \times 100$ (Figure 8c), between the calculated survival probability and the two-exponential fit depend both on time and on the base concentration. At short times it is positive and its value increases with the concentration from 1.2% at 0.5 M NaAc to 7.5% at 4 M NaAc. From Figure 8 it is clearly seen that the two-exponential function fails to fit the calculated survival probability even though the deviations are relatively small. The value of the short-time rate constant k_1 is close to $k_0 e^{-\beta U(a)}$, while the long-time rate constant is close to k_D. Using ordinary homogeneous chemical kinetic equation formalism generates a sum of exponents. $S'(t)$ fits the data better than a biexponential function. The signal-to-noise ratio of the experimental results and the contributions of other components to the signal prevents us from showing that the experimental signal fits only to $S(t)$ and not to other functional forms.

The electrostatic potential $U(a)$ affects the rate of the reaction between the acid and the base, in our case the repulsion between the acetate negative ion and the triply negative charged HPTS. $U(a)$ affects both the initial rate constant, $k_0 e^{-\beta U(a)}$, and the effective contact radius a_e (eq 7). a_e affects both the diffusion-limited rate constant, $k_D = 4\pi D a_e N'$, and the parameter γ (eq 6), which affects the time dependence of $k(t)$ (eq 3). The Debye−Hückel ionic atmosphere decreases this repulsion. The screening effect depends strongly on the acetate concentration (eqs 4−5). The larger the acetate concentration, the larger the screening. Figure 9 shows the concentration dependence of the initial rate constant. As can be seen the initial rate constant increases by a factor of 2 from 0.5 to 4 M.

The exact mechanism of proton transfer from ROH* to the solvent and/or to a specific base like in this study is not yet determined. The rate of intermolecular proton transfer is correlated with the difference in the acid−base properties of the proton donor and acceptor, respectively. Pines and co-workers found such a correlation.[18] The basic assumption for such free energy correlation is that within a family of similar reactions the intrinsic free energy barrier for the reaction is modified by the total free energy change ΔG.[33] The free energy barrier for the reaction, G_a, is then assumed to depend on some intrinsic barrier G_a^0 and ΔG. G_a^0 is the activation energy for the case $\Delta G = 0$ (the symmetric case). They found that the measured proton-transfer rates correlate with an Arrhenius plot

$$k_d = k_d^0 \exp(-G_a/RT) \tag{13}$$

where $k_d^0 = 3 \times 10^{11}$ s^{-1} is the activationless rate limit and $G_a^0 = 2.9$ kcal/mol. The value $(k_d^0)^{-1}$ is between $\tau_L < k_d^{-1} < \tau_D$, where $\tau_L = \varepsilon_\infty/\varepsilon_0$, and τ_D is the longitudinal relaxation time. ε_∞ and ε_0 are the high- and low-frequency dielectric constants, respectively. From the Pines and co-workers study,[18] one expects to find an upper limit to the water-mediated proton-transfer reaction rate constant. This limit should be k_d^0, and the time for the proton-transfer process should not be shorter than ~3 ps. If the proton-transfer rate depends on the solvation dynamics and hydrogen-bond dynamics as rate-limiting steps for the actual proton-transfer process, then we expect that the proton-transfer rate will not be shorter than $(2.2 \text{ ps})^{-1}$ for HPTS according to the Tran-Thi study.[20] In this study the shortest pseudo first-order rate constant for the direct proton transfer to a base molecule was found to be $ck_0 e^{-\beta U(a)} = 3.2 \times 10^{11}$ s^{-1} (at 4 M NaAc). This rate constant is within the limit of the prediction of Pines at al.[18]

Long-Time Behavior. We extended the time scale of observation of the chemical reaction ROH* + B$^-$ → RO$^-$* + HB to the nanosecond scale by measuring the time-resolved fluorescence using the time-correlated single-photon counting (TCSPC) technique. The TCSPC technique has a relatively poor

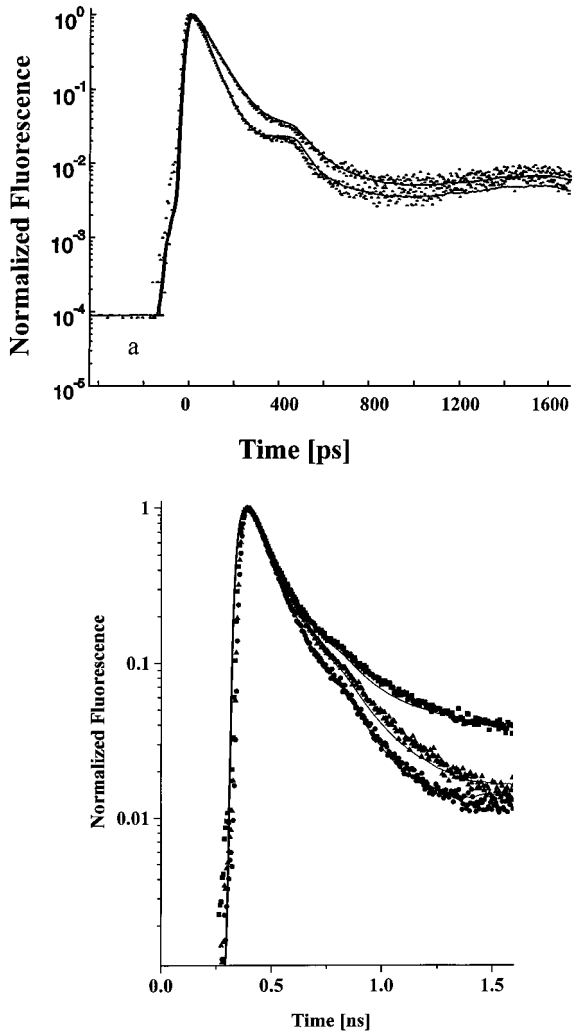

Figure 10. Time-correlated single photon counting signal of HPTS−H_2O solutions in the presence of NaAc salt at various concentrations (dots) along with the computer fits (solid line). (a, top) Moderate salt concentrations, top to bottom: 0.5, 1 M NaAc. (b, bottom) Low salt concentrations, top to bottom: neat water (■), 0.03 M (▲), 0.12 M NaAc (●).

time resolution, and our system instrument response function (IRF) is limited to 45 ps. The signal/noise ratio is excellent and the dynamic range is large, about 4 decades. Time-resolved fluorescence measurements were used extensively in the last two decades to study photoacid proton-transfer reactions. In this section we will show that both techniques using different pulse widths, intensity, and time scales produce the same information on the photoacid−base reactions.

Figure 10a shows on a semilog scale the time-resolved emission measured at 435 nm of HPTS aqueous solutions containing sodium acetate at moderate concentrations of 0.5 and 1.0 M. The fluorescence band maximum of the ROH* emission is at 440 nm. We measured the luminescence at 435 nm to reduce the overlap between the ROH* and the RO^-* emission bands (RO^-* maximum is at 510 nm). We fit the experimental emission decay using eqs 2−8 and convolute the calculated $S(t)$ (eq 8) with the IRF of the experimental system. The fits are shown as solid lines in Figure 10.

As can be seen from Figure 10a, the fit to the experimental data is good for both 0.5 and 1 M salt concentrations. We used for the computer fit the same parameters as for the ultrashort pump−probe experiments (Table 1). We find a small fluorescence background with an amplitude of about 0.001 of the signal

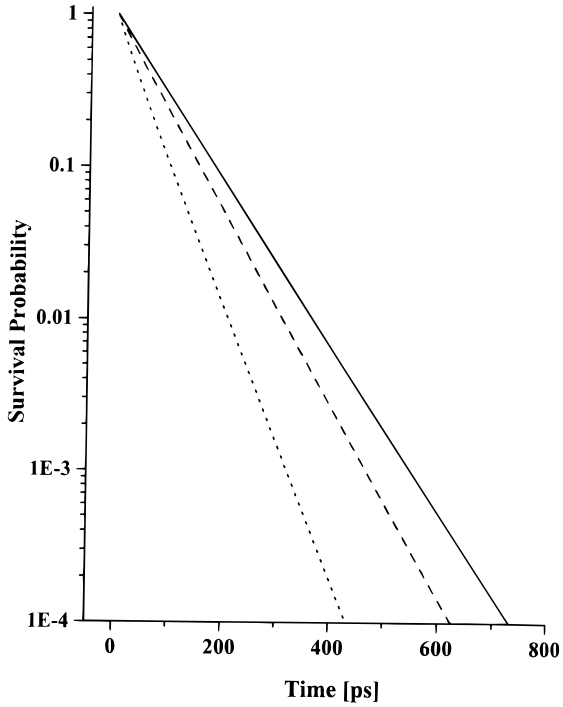

Figure 11. Calculated survival probabilities of ROH*, $S(t)$, at different NaAc concentrations; top to bottom: 0.12, 0.5, and 1.0 M.

maximum, which we attribute to the presence of NaAc in the solution. At low NaAc concentrations (0.03−0.5 M), we used successfully the Debye−Hückel screening potential, eqs 4−5. We found that we cannot achieve a good fit to the experimental signal of 1 M NaAc with the calculated screening length κ_{DH}^{-1} (eq 5c), where $B = 3.2 \times 10^{-9}$ cm^{-1} mol$^{-0.5}$. We got a good fit when we used $B = 2.9 \times 10^{-9}$ cm^{-1} mol$^{-0.5}$ (see Figure 10a); i.e., the effective screening at high concentrations ($c > 1$ M) is smaller than that predicted by the Debye−Hückel theory.

Figure 10b shows the experimental data along with the computer fit of HPTS solutions at low acetate concentrations. The top plot shows the result for the HPTS emission in neat water. The large difference of this signal compared to 0.03 and 0.12 M NaAc solutions arises from the contribution of the proton geminate recombination process to the emission tail of ROH* in neat water.[12−15] Note that the experimental decay curves at these concentrations are almost identical. Introducing to the aqueous solution an amount of acetate larger than ∼0.03 M strongly reduces the geminate recombination (see Figure 10b) since the acetate anion efficiently reacts with the ejected proton, $H^+ + Ac^- \rightarrow$ HAc. The proton diffusion is high, and therefore the second-order diffusion-limited reaction rate constant, $k_D^{H+} = 4\pi D_{H^+} a_e N'$, for this reaction is 5×10^{10} M^{-1} s^{-1}.[3]

At low NaAc concentrations (0.03 and 0.12 M), the computer fit is almost identical for all the concentrations. At such low concentrations the pseudo first-order rate constant $k'_D = k_D[Ac^-]$ is much smaller than the direct proton-transfer rate constant from ROH* to water, $k_D = 8 \times 10^9$ s^{-1}. For acetate concentration of 0.1 M, $k_D \sim 3 \times 10^9$ M^{-1} s^{-1} and $k'_D = 3 \times 10^8$ s^{-1}. This value is smaller by an order of magnitude than k_d, and hence the acid−base reaction is inefficient to compete with the proton transfer to the solvent. We find that the experimental data at long times deviates from the computed signal. The reason is that at these low concentrations the proton geminate recombination contributes to the experimental signal. We plan to include in future model calculations the repopulating process RO^-* + $H^+ \rightarrow$ ROH* and other processes that occur

in solution and compete with the main process—the photoacid−base neutralization. At acetate concentrations larger than 0.1 M, the direct photoacid−base reaction competes effectively with the proton transfer to water and the decay rate of ROH* emission increases.

Figure 11 shows the survival probability of ROH* at long time. From Figure 6 one can see that $k(t)$ at times of about 50 ps assumes approximately the asymptotic value given by eq 12. As mentioned in the previous section, since $k_0 \gg k_D$, then at long times (>50 ps) $k \approx k_D = 3 \times 10^9\ M^{-1}\ s^{-1}$. At long times $S'(t)$ decays almost exponentially with an effective rate constant $k' = k_D[Ac^-] + k_d$ as can be clearly seen in Figure 11.

Summary

Pump−probe techniques with ∼150 fs resolution and time-resolved emission with ∼20 ps resolution were employed to measure the photoacid−base reaction rate. Excited 8-hydroxypyrene-1,3,6-trisulfonate (HPTS) reacted with acetate anion in aqueous solution. We used a diffusive model to describe the reaction kinetics. We found a good agreement between the model calculations and the experimental data. We have found relatively large intrinsic rate constant $k_0 = 1.6 \times 10^{11}\ M^{-1}\ s^{-1}$ for the reaction. This rate constant is about 20 times larger than the diffusion-limited rate constant. In such a case the overall reaction rate coefficient is ∼20 times larger at $t = 0$ than at $t \rightarrow \infty$ and the survival probability decays nonexponentially. The isotope effect $k_0^{H+}/k_0^{D+} \cong 4$ is about the same as that of direct proton transfer to water itself.

Acknowledgment. We thank Prof. N. Agmon and Dr. E. Pines for helpful discussions. This work was supported by grants from the Israel Science Foundation and the James−Franck German−Israel Program in Laser matter interaction.

References and Notes

(1) Förster, T. *Elektrochem.* **1950**, *54*, 531.
(2) Weber, K. *Phys. Chem. B* **1931**, *15*, 18.
(3) Weller, A. *Prog. React. Kinet.* **1961**, *1*, 187.
(4) Beens, H.; Grellmann, K. H.; Gurr, M.; Weller, A. H. *Discuss. Faraday Soc.* **1965**, *39*, 183.
(5) Ireland, J. F.; Wyatt, P. A. H. *Adv. Phys. Org. Chem.* **1976**, *12*, 131.
(6) Martinov, I. Y.; Demyashkevitch, A. B.; Uzhinov, B. M.; Kuzmin, M. G. *Russ. Chem. Rev.* (*Usp. Khim.*) **1977**, *46*, 3.
(7) Schulman, E. F. *Fluorescence and Phosphorescence Spectroscopy*; Pergamon Press: New York, 1977.
(8) Arnout, L. G.; Formosinho, S. J. *J. Photochem. Photobiol. A* **1993**, *75*, 1.
(9) Wan, P.; Shukla, D. *Chem. Rev.* **1993**, *93*, 571.
(10) Knochenmuss, R. *Chem. Phys. Lett.* **1998**, *293*, 191.
(11) Peters, K. S.; Cashin, A.; Timbers, P. *J. Am. Chem. Soc.* **2000**, *122*, 107.
(12) Pines, E.; Huppert, D. *J. Chem. Phys.* **1986**, *84*, 3576.
(13) Pines, E.; Huppert, D.; Agmon, N. *J. Chem. Phys.* **1988**, *88*, 5620.
(14) Agmon, N.; Pines, E.; Huppert, D. *J. Chem. Phys.* **1988**, *88*, 5631.
(15) Huppert, D.;Pines, E.; Agmon, N. *J. Opt. Soc. Am.* **1990**, *7*, 1500.
(16) Goldberg, S. Y.; Pines, E.; Huppert, D. *Chem. Phys. Lett.* **1992**, *192*, 77.
(17) Gösele, U. M. *Prog. React. Kinet.* **1984**, *13*, 63.
(18) Pines, E. Magnes, B-Z.; Lang, M. J.; Fleming, G. R. *Chem. Phys. Lett.* **1997**, *281*, 413.
(19) Eigen, M. *Angew. Chem., Int. Ed. Engl.* **1964**, *3*, 1.
(20) Prayer, C.; Gustavsson, T-H. Tran-Thi, In *Fast Elementary Processes in Chemical and Biological Systems*; American Institute of Physics: Woodbury, NY, 1996; Vol. 364, pp 333−339.
(21) Backus, S.; Peatross, J.; Huang, C. P.; Murnane, M. M.; Capteyn, H. C. *Opt. Lett.* **1995**, *20*, 2000.
(22) Von Smoluchowski, M. *Ann. Phys.* **1915**, *48*, 1103.
(23) Szabo, A. *J. Phys. Chem.* **1989**, *93*, 6929.
(24) Robinson, R. A.; Stokes, R. H. *Electrolyte solutions*, 2nd ed.; Butterworths: London, 1959.
(25) Solntsev, K. M.; Huppert, D.; Tolbert, L. M.; Agmon, N. *J. Am. Chem. Soc.* **1998**, *120* (31), 7981.
(26) Solntsev, K. M.; Huppert, D.; Agmon, N. *J. Phys. Chem.* **1999**, *103*, 6984.
(27) Jimenez, R.; Fleming, G. R.; Kumar, P. V.; Maroncelli, M. *Nature* **1994**, *309*, 471.
(28) Zichi, D. A.; Rossky, P. J. *J. Chem. Phys.* **1986**, *84*, 2814.
(29) Skaf, M. S.; Ladanyi, B.M. *J. Phys. Chem.* **1996**, *100*, 18, 258.
(30) Zolotov, B.; Gan, A.; Fainberg, B. D.; Huppert, D. *J. Lumin.* **1997**, 72−74, 842.
(31) Bertolini, D.; Cassettari, M.; Salvetti, G. *J. Chem. Phys.* **1982**, *76*, 3285.
(32) Agmon, N.; Levine, R. D. *Chem. Phys. Lett.* **1977**, *52*, 197.
(33) Conway, B. H. In *Modern Aspects of Electrochemistry*; Bockris, J. M., Conway, B. H., Eds.; Butterworths: London, 1964; Vol. 3.
(34) Kwart, H. *Acc. Chem. Res.* **1982**, *15*, 401.
(35) Bell, R. P. *The Proton in Chemistry*; Cornell University Press: Ithaca, NY, 1973.